

SUPERPOSITION OF FREE AND BOUND EXCITON EMISSION SPECTRA IN $\text{ZnP}_2\text{-D}_4^8$

I. G. Stamov¹, N. N. Syrbu², V. V. Ursaki³, and Yu. Ivanenco²

¹*Tiraspol State Corporative University, Yablocikin str. 5, Tiraspol, 2069 Republic of Moldova*

²*Technical University of Moldova, Stefan cel Mare str. 168, Chisinau,
MD-2004 Republic of Moldova*

³*Institute of Applied Physics of the Academy of Sciences of Moldova, Academiei str. 5, Chisinau,
MD-2028 Republic of Moldova*

(Received 10 September 2011)

Abstract

Bound exciton lines are found in the luminescence spectra of Mn, Sn, Cd, and Sb doped tetragonal zinc diphosphide crystals at the temperature of 10 K. Zero phonon lines of bound and free exciton emission, as well as their phonon replica, are identified in the spectra. The emission lines are described in terms of levels of an axial center. The superposition of luminescence due to free excitons and excitons bound to the axial center is investigated in detail. The amplification of lines associated with forbidden transitions of bound excitons is observed in the region of phonon replica of free exciton recombination.

1. Introduction

The $\text{ZnP}_2\text{-D}_4^8$ compound is an indirect band semiconductor with a bandgap of 2.21 eV at 10 K. The $\text{ZnP}_2\text{-D}_4^8$ crystals demonstrate a strong birefringence and bright luminescence as well as a high photosensitivity [1-7]. Active elements, such as p-n junctions, Schottky diodes, optical pulse switches, etc., are elaborated on the basis of these crystals, which are also promising for polarization sensitive optoelectronic devices.

In this paper, we present new data concerning the fine structure of absorption and luminescence spectra of undoped and Mn, Sn, Cd, and Sb doped tetragonal zinc diphosphide crystals at 10 K. The superposition of luminescence due to free excitons and excitons bound to the axial center is observed in ZnP_2 crystals.

2. Experimental

The CuAlSe_2 crystals with $2.5 \times 1.0 \text{ cm}^2$ mirror surfaces and 300 – 400 μm thickness were grown by vapor phase transport. The surface of some platelets were parallel to the C axis. The optical transmission and reflectivity spectra were measured with a MDR-2 spectrometer. The samples were mounted on the cold station of an LTS-22 C 330 optical cryogenic system for low-temperature measurements.

3. Results and discussion

Optical properties of tetragonal zinc diphosphide were reported in a number of papers, the indirect character of the bandgap being established and the energy of E_g and optical phonons being determined [5-9]. A stepwise structure was revealed in the absorption spectra measured in $E \parallel c$ and $E \perp c$ polarizations in the region of low values of the absorption coefficient. The absorption edge is well described by the $K(h\nu)$ dependence characteristic of allowed indirect transitions. The threshold value of the zero-phonon indirect transition in the exciton band E_{g1} equals 2.21 eV. A stepwise absorption due to emission of phonons is observed in this region [5, 6]. Direct allowed transitions are observed in the region of high values of the absorption coefficient. The direct bandgap E_g^d at 2 K equals 2.40 eV [5, 6].

Figure 1 presents the photoluminescence spectra of undoped and Mn doped $ZnP_2 - D_4^8$ crystals measured at 10 K in the region of the absorption edge. A weak E_{ext}^L luminescence peak is observed at 2.2085 eV, which is due to emission from the free exciton level. The features x_1-x_{10} in the spectrum correspond to the optical phonon replica of the free exciton emission band $E_{gx}^{\text{lib}} = 2.2085$ eV (see Table 1) [10-14]. Narrow lines due to various optical phonon replica of the bound exciton emission were observed in the luminescence spectra of $ZnP_2 - D_4^8$ [5-7, 16] and $CdP_2 - D_4^8$ [15] crystals.

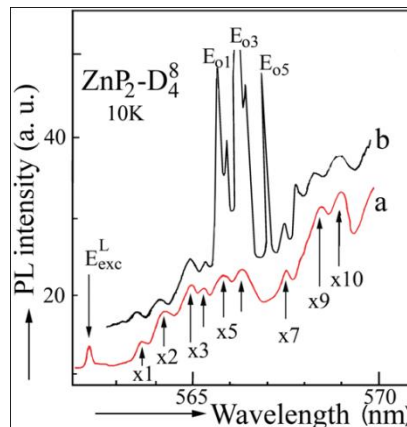


Fig. 1. Emission spectra of undoped (a) and Mn-doped (b) $ZnP_2 - D_4^8$ crystals measured at 10 K.

The unit cell of ZnP_2 crystals with the D_4^8 (D_4^4) space group contains 8 formula units, i.e., 24 atoms, and the number of phonon branches equals 72 [10-13]. Due to this large number of vibration modes, one can observe the luminescence of free excitons with the emission of many phonons. Narrow $E_{01}-E_{05}$ lines and weaker x_1-x_{10} lines are observed in the luminescence spectra of Mn-doped $ZnP_2 - D_4^8$ crystals (curve b in Fig. 1). The X_i lines are the phonon replica of the free exciton emission line. These lines are observed simultaneously with the narrow $E_{01}-E_{05}$ lines associated with excitons bound to the Mn impurity atom. E_{01} (2.1951 eV), E_{02} (2.1944 eV), E_{03} (2.1928 eV), E_{04} (2.1927 eV), and E_{05} (2.1898 eV) zero phonon lines of the bound exciton very narrow. The x_i lines are two orders of magnitude weaker, and their width is an order of magnitude larger as compared to the $E_{01} - E_{05}$ lines. These two types of lines x_i and $E_{01} - E_{05}$ are

observed simultaneously in the same energy interval (Fig. 1).

Table 1. Energies of indirect transitions of the free excitons determined at 10 K from the absorption and photoluminescence spectra in $\text{ZnP}_2 - D_4^8$ crystals

Absorption	Polarization E c [5-7]			Polarization E⊥c [5-7]		
	Peak label	Energy position of peak, eV	Phonon energy, meV	Peak label	Energy position of the peak, eV	Phonon energy, meV
	E_{gx}	2.2085		E_{gx}	2.2085	
	a_1	2.2180	9.5	b_1	2.2168	8.3
	a_2	2.2210	12.5	b_2	2.2204	11.9
	a_3	2.2238	15.3	b_3	2.2232	14.7
Luminescence	Unpolarized light					
	E_{gx}	2.2085	Phonon energy, meV			
	x_1	2.2002	8.3			
	x_2	2.1975	11.0			
	x_3	2.1941	14.4			
	x_4	2.1937	14.8			
	x_5	2.1913	17.2			
	x_6	2.1900	18.0			

It is known that at thermodynamic equilibrium and assuming the absence of degeneracy, the rate of radiative recombination is given by the correlation [15]:

$$R = \frac{8\pi k_B^3 T}{c^2 h^3} \int_0^\infty \frac{n^2 U^2 K du}{e^u - 1}, \quad (1)$$

where k_B is the Boltzmann constant, c is the speed of light, h is the Planck constant, T is the temperature, n is the carrier concentration, k is the absorption coefficient, $U = \frac{h\nu}{k_B \pi}$. It follows

from this formula that transitions contributing to the recombination and to the absorption coefficient are the same.

The spectral distribution of the absorption for indirect transitions in the excitonic band with the absorption and emission of phonons is determined by the formula

$$K(\hbar\omega) = \frac{A(\hbar\omega - E_g + E_{p1} + G_{ext1})^2}{e^{E_{p1}/kT} - 1} + \frac{A(\hbar\omega - E_g - E_{p1} + G_{ext1})^2}{1 - e^{-E_{p1}/kT}} + \frac{A'(\hbar\omega - E_g + E_{p2} + G_{ext2})^2}{e^{E_{p2}/kT} - 1} + \frac{A'(\hbar\omega - E_g - E_{p2} + G_{ext2})^2}{1 - e^{-E_{p2}/kT}} \quad (2)$$

The first two terms determine the indirect transitions with the absorption and emission of a phonon E_{p1} to the excitonic band G_{ext1} , while the last two terms determine the indirect transitions with the absorption and emission of a phonon E_{p2} to the excitonic band G_{ext2} . Expression (2) suggests that both transitions to the G_{ext1} and G_{ext2} excitonic bands are possible simultaneously provided that

$$E_{p1} = G_{ext1} - G_{ext2} + E_{p2} \quad (3)$$

The indirect transitions with the absorption of phonons are determined by the following

terms:

$$K(\hbar\omega) = \frac{A(\hbar\omega - E_g + E_{p1} + G_{\text{ext1}})^2}{e^{E_{p1}/kT} - 1} + \frac{A'(\hbar\omega - E_g + E_{p2} + G_{\text{ext2}})^2}{e^{E_{p2}/kT} - 1} = K_{a1}(\hbar\omega) + K_{a2}(\hbar\omega) \quad (4)$$

The transition described by the two terms represents two independent processes occurring in the first and the second excitonic bands, respectively. The absorption with the emission of two and more phonons in one excitonic band is described by the following expression:

$$K_e(\hbar\omega) = \frac{A(\hbar\omega - E_{gx} + E_{p1} + G_{\text{ext1}})^2}{e^{E_{p1}/kT} - 1} + \frac{A'(\hbar\omega - E_{gx} + E_{p2} + G_{\text{ext2}})^2}{e^{E_{p2}/kT} - 1} + \dots \quad (5)$$

In $\text{ZnP}_2\text{-D}_4^8$ crystals at the temperature of 10 K, the energy difference between the levels of the free (G_{ext1}) and bound E_0^1 (G_{ext2}) excitons equals 13.3 meV, while the energy of the optical phonons reaches the value of 59.5 meV. Therefore, the condition $E_{p1} = G_{\text{ext1}} - G_{\text{ext2}} + E_{p2}$ is satisfied by the levels of the bound and free excitons, and the process of recombination emission occurs simultaneously from the two centers. The emission due to the dissociation of free excitons leads to the emergence of a number of (x_i) bands in the long-wavelength region from the $E_{\text{ext}}^{\text{lib}}$ (2.2085 eV) band at the distance equal to the energy of optical phonons.

Figure 2 presents the energy diagram of exciton levels of an exciton bound to the axial center. The narrow lines $E_0^1 - E_0^5$ are due to zero-phonon lines of the exciton bound to the axial center [5, 6]. An exciton composed of an electron with spin $1/2$ and a hole with spin $3/2$ forms two levels (Σ and Π) from the level $J = 1$ [15,16]. The state $J = 2$ splits into three levels Σ , Π , and Δ under the action of axial field and spin-orbit interaction. The energy separation between $\Sigma(\Pi) - \Delta$ states determines the value of level splitting due to spin-orbit interaction (Δ_{so}). In this model, the value of the splitting due to spin-orbit interaction can be larger or smaller than the value of the splitting due to the crystal field. The lines E_0^3 and E_0^4 are the most intensive among the $E_0^1 - E_0^5$ group of lines. That means that the E_0^3 and E_0^4 emission lines are due to allowed transitions from bands with Σ and Π ($J = 1$) symmetry to the ground state, respectively. These lines are split with a value of around 0.1 meV (Figs. 1, 2). The lines E_0^1 and E_0^2 are split by 0.75 meV, and they are less intensive than the E_0^3 and E_0^4 lines. The lines E_0^1 and E_0^2 are due to transitions from the Σ and Π levels of the forbidden bound exciton state (Fig. 2). These levels are split by the crystal field of the axial center the exciton is bound to. The energy interval between the $\Sigma - \Sigma$ levels is 2.2 meV. The obtained intensity of luminescence lines and their energy position indicate that the value of the spin-orbit splitting is larger than the splitting due to the crystal field (Fig. 2). Two allowed intensive emission lines should be observed with a model of excitons bound to the axial center. These lines should be observed in the short-wavelength region of the spectrum. The luminescence lines due to the selection rule for forbidden transitions could be observed as weak lines. The situation can change if the energy of the photon emitted as a result of annihilation of the free exciton with the emission of a phonon corresponds to the energy of the bound exciton forbidden transition. This can lead to a resonant excitation of forbidden states of the bound excitons and to the lifting of the prohibition imposed by the selection rule which should result in the intensification of corresponding luminescence lines [3]. One can see from the experiment that an emission line is observed at 2.1951 eV, which could be attributed to a phonon replica of the free exciton emission. The energy of this emission line differs from the

E_{gx} energy by the energy of the optical phonon (13.3 meV). On the other hand, this line (2.1951 eV) coincides with the energy position of the bound exciton level E_0^1 (2,1951 eV), and it is close to the E_0^2 (2,1944 eV).

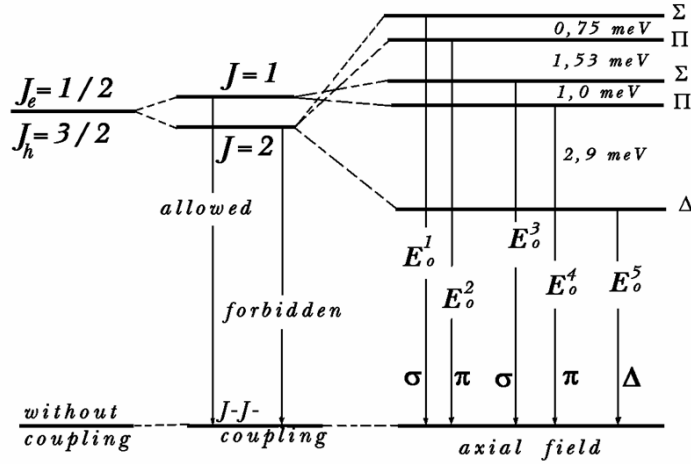


Fig. 2. Energy levels and transitions related to excitons bound to an axial Mn center in $ZnP_2-D_4^8$ crystals.

ZnP_2 crystals doped with Sn, Cd, and Sb also demonstrate bright luminescence. Narrow emission lines, as well as broader lines, are observed in these crystals. Figure 3 presents sections of spectra containing zero-phonon luminescence lines of excitons bound to these impurities. These spectra were measured under identical experimental conditions in crystals doped with these impurities. Phonon replicas are also observed in addition to the zero-phonon lines. Figure 4 presents luminescence spectra of the $ZnP_2-D_4^8$ crystals doped with Sn and Cd measured at 10 K. Zero phonon lines of excitons bound to Sn atoms (F_{01}, F_{02}, F_{03}) as well as phonon replicas f_1, f_2, \dots, f_5 are observed in these spectra. A large number of bands are also observed in the long-wavelength side of the f_5 line (not shown in this figure). A group of intensive narrow lines $D_{01}, D_{02}, D_{03}, D_{04}$, as well as weaker d_1-d_n lines, are observed in crystals doped with Cd (four of these lines are shown in Fig. 4).

The narrow intensive D_{01}, D_{02}, D_{03} , and D_{04} lines in $ZnP_2-D_4^8$ crystals doped with Cd are also due to excitons bound to the axial center of Cd. The d_1-d_n lines are phonon replicas of the $D_{01}, D_{02}, D_{03}, D_{04}$ lines. These data demonstrate that the centers involved have identical parameters. The energy interval $\Sigma - \Sigma$ is the following: 2.28 meV in crystals doped with Mn ($E_0^1 - E_0^3$), 2.0 meV in crystals doped with Sn ($F_{01}-F_{03}$), and 2.3 meV in crystals doped with Cd ($D_{01}-D_{03}$). One can see that the splitting of the states of the electron with a spin $J_e=1/2$ and the holes with a spin $J_h=3/2$ due to the crystal field practically coincide for the three considered centers.

Two groups of lines are present in the long-wavelength region of luminescence spectra of $ZnP_2 - D_4^8$ crystals doped with Sb as previously reported [6, 7]. The narrow intensive emission lines A_0^1 (2.1444 eV) and A_0^2 (2.1442 eV) are zero-phonon lines of excitons bound to the axial center, and are due to transitions from the Σ, Π ($J=1$) levels to the ground state. These lines are split by 0.22 meV. The weak luminescence lines B_0^1 (2.1422 eV), B_0^2 (2.1417 eV), and B_0^3 (2.1400 eV) are due to forbidden transitions from the Σ, Π , and Δ ($J=3/2$) levels to the

ground state (Fig. 5). The emission lines a_1, a_2, \dots, a_{18} are phonon replicas of the A_0^1 and A_0^2 lines. The $B_0^1, B_0^2,$ and B_0^3 lines are weak, since removal of prohibition due to participation of phonons does not occur in these spectra. Apart from that, the $B_0^1, B_0^2,$ and B_0^3 emission lines are situated in the long-wavelength region from the A_0^1 and A_0^2 lines. Therefore, the value of the spin-orbit splitting is lower than the crystal field splitting in the band model of this center. The splitting of the $J=1$ and $J=3/2$ states deduced from the energy difference between the A_0^1 and B_0^1 levels is equal to 2.2 meV. The scheme of electronic transitions responsible for the emission lines is shown in Fig. 5. The lines b_0^1 (2.0212 eV) and b_0^2 (2.0210 eV) observed in the long-wavelength region, which were also previously reported [16], are zero-phonon lines of excitons bound to another axial center. The phonon replicas of these lines are also observed in Fig. 5 similarly to previous data [16].

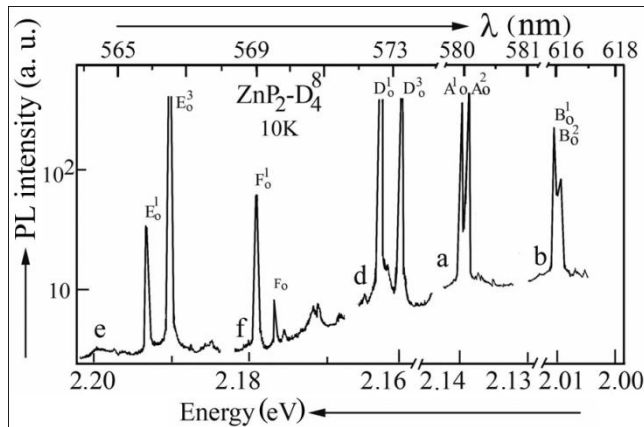


Fig. 3. Sections of the luminescence spectra containing the most intensive lines at 10 K for $ZnP_2-D_4^8$ crystals doped with Mn (curve e), Sn (curve f), Cd (curve d), Sb (curves a and b). Levels and transitions related to excitons bound to an axial Mn center in $ZnP_2-D_4^8$ crystals.

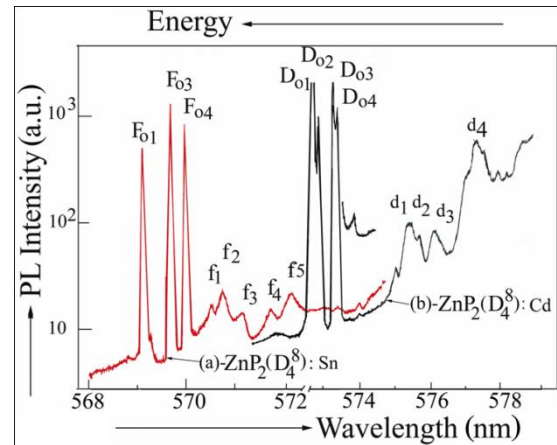


Fig. 4. Luminescence spectra of $ZnP_2-D_4^8$ crystals doped with Sn and Cd measured at 10 K.

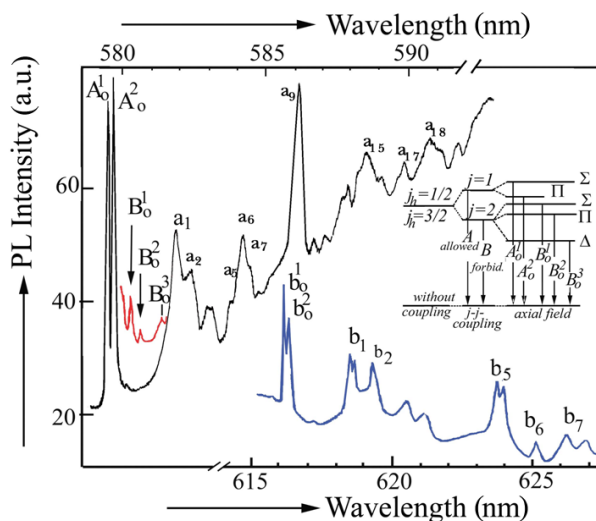


Fig. 5. Luminescence spectra of $ZnP_2-D_4^8$ crystals doped with Sb measured at 10 K.

3. Conclusions

The luminescence spectra of the tetragonal modification of zinc diphosphide crystals doped with Mn, Sn, Cd, and Sb are described by allowed and forbidden recombination transitions in the model of axial center levels. The superposition of the luminescence from free and bound excitons enhances the emission lines related to forbidden recombination transitions of excitons bound to axial centers. The amplification of the emission from levels of forbidden transitions of bound excitons occurs when the energy of the photon emitted as a result of annihilation of the free exciton with the emission of a phonon coincides with the energy of the bound exciton forbidden transition.

References

- [1] O. Arimoto, Y. Imai, S. Nakanishi, and H. Itoh, *J. Luminescence* 108, 201, (2004).
- [2] N. N. Syrbu and I. G. Stamov, *Fiz. Tekhn. Polupr.* 25, 2115, (1991).
- [3] K. Nakamura, K. Ohya, and O. Arimoto, *J. Luminescence* 94-95, 393, (2001).
- [4] O. Arimoto, S. Umamoto, and K. Nakamura, *J. Luminescence* 87-89, 284, (2000).
- [5] N. N. Syrbu, *Optoelectronic properties of A²B⁵ compounds*, Stiintsa, Kishinev (1983).
- [6] N. N. Syrbu, V. I. Morozova, and G. I. Stratan, *Fiz. Tekhn. Polupr.* 23, 1771, (1989).
- [7] N. N. Syrbu, V. I. Morozova, and G. I. Stratan, *Fiz. Tekhn. Polupr.* 26, 74, (1992).
- [8] N. N. Syrbu, I. G. Stamov, V. I. Morozova, V. K. Kiossev, and L. G. Peev, *Proc. Ist Int Symp. Phys. Chem. II-V Comp., Mogilany, Poland* 237 (1980).
- [9] I. S. Gorbani, V. A. Gorinya, V. I. Lugovoi, and A. P. Makovetskaia, *Fiz. Tekhn. Polupr.* 17, 1638, (1975).
- [10] N. N. Syrbu, I. G. Stamov, and A. I. Kamertsel, *Fiz. Tekhn. Polupr.* 26, 1191, (1992).
- [11] N. Sobotta, H. Neumann, V. Riede, and N. Syrbu, *Solid St. Commun.* 48, 297, (1992).
- [12] N. N. Syrbu and V. E. Livin, *Fiz. Tekhn. Polupr.* 25, 1765, (1991).
- [13] N. N. Syrbu and V. E. Livin, *Fiz. Tekhn. Polupr.* 25, 238, (1991).
- [14] N. N. Syrbu and V. E. Livin, *Fiz. Tekhn. Polupr.* 24, 1911, (1990).
- [15] R. Bindemann, H. Fisher, K. Kreher, and N. N. Syrbu, *Phys. St. Sol. (b)* 69, K79 (1975).
- [16] J. J. Hopfield, P. J. Dean, and D. G. Thomas, *Phys. Rev.* 158, 748, (1967).